

V.F. Bolyukh, A.I. Kocherga, S.V. Oleksenko, I.S. Schukin

## A TECHNIQUE OF EXPERIMENTAL INVESTIGATIONS OF LINEAR IMPULSE ELECTROMECHANICAL CONVERTERS

*Purpose.* Development of a technique of experimental studies linear pulse electromechanical converters parameters, which are used as shock-power devices and electromechanical accelerators, and comparing the experimental results with the calculated indices obtained using the mathematical model. *Methodology.* Method of experimental investigations of linear electromechanical converter is that the electrical parameters are recorded simultaneously (inductor winding current) and mechanical parameters characterizing the power and speed indicators of the yoke with actuator. Power indicators are primarily important for shock-power devices, and high velocity – for electromechanical accelerators. Power indices were investigated using piezoelectric sensors, a system of strain sensors, pressure pulsation sensor and high-speed videorecording. Velocity indicators were investigated using a resistive movement sensor which allows to record character of the armature movement with actuating element in each moment. *Results.* The technique of experimental research, which is the simultaneous recording of electrical and mechanical power and velocity parameters of the linear electromechanical converter pulse, is developed. In the converter as a shock-power device power indicators are recorded using a piezoelectric transducer, strain sensors system, pressure pulsation sensor and high-speed video. The parameters of the inductor winding current pulse, the time lag of mechanical processes in relation to the time of occurrence of the inductor winding current, the average speed of the yoke, the magnitude and momentum of electrodynamic forces acting on the plate strikes are experimentally determined. In the converter as an electromechanical accelerator velocity performance recorded using resistive displacement sensors. It is shown that electromechanical converter processes have complex spatial-temporal character. The experimental results are in good agreement with the calculated figures obtained by means of a mathematical model that describes the ultrafast electromagnetic, thermal and mechanical processes that occur when the yoke moves relative to the inductor. *Originality.* For the first time offered during experimental studies of impulse linear electromechanical converter to both to measure the electrical parameters, namely the inductor winding current, and mechanical parameters characterizing the power and velocity performance with yoke actuator. *Practical value.* The technique of experimental investigations the parameters of the linear pulse electromechanical converter that can be used to investigate the shock-power devices and electromechanical accelerators is proposed. References 13, figures 18.

*Key words:* linear impulse electromechanical converter, shock-power device, electromechanical accelerator, experimental investigations technique, mathematical model.

*Разработана методика экспериментальных исследований, которая состоит в одновременной регистрации электрических и механических силовых и скоростных параметров линейного импульсного электромеханического преобразователя. При работе преобразователя в качестве ударно-силового устройства силовые показатели регистрируются с использованием пьезодатчика, системы тензодатчиков, датчика пульсации давления и скоростной видеосъемки. При работе преобразователя в качестве электромеханического ускорителя скоростные показатели регистрируются с использованием резистивного датчика перемещений. Показано, что электромеханические процессы в преобразователе носят сложный пространственно-временной характер. Результаты экспериментальных исследований удовлетворительно согласуются с расчетными показателями, полученными при помощи математической модели, которая описывает быстропротекающие электромагнитные, тепловые и механические процессы, возникающие при перемещении якоря относительно индуктора. Библи. 13, рис. 18. Ключевые слова: линейный импульсный электромеханический преобразователь, ударно-силовое устройство, электромеханический ускоритель, методика экспериментальных исследований, математическая модель.*

**Introduction.** Linear impulse electromechanical converters (LIEC) are designed to create shock-mechanical pulses to the object of action with little movement of the actuating element (AE) or to accelerate it on a short active site [1]. These converters are used in many branches of science and technology as shock-power devices and electromechanical accelerators.

Electromagnetic hammers and pile driving devices are used in the construction industry, ratchet beaters and vibrators in the mining industry, vibration seismic sources in geological exploration, presses and hammers with a large range of impact energy in the engineering industry, vibration mixers and dispensers in the chemical and medical-biological industry.

LIEC are also used in high-speed valve and switching equipment, in test complexes for testing critical equipment for impact loads, in magnetic-pulse devices for pressing ceramics powders, cleaning containers from sticking loose materials, destroying information on digital media, etc. [2-4].

The inductive-type LIEC provide a non-contact movement of the electrically conductive armature with respect to a stationary inductor driven from a pulsed source, for example, capacitive energy storage (CES) with an electronic current pulse generation system [5]. In it, there are rapid electromagnetic, thermal and mechanical processes that occur when the yoke is moved rapidly in an environment.

Mathematical models of LIEC are realized, as a rule, using either chain or field representations [6, 7]. This raises the question of the correspondence between the parameters of the LIEC obtained by calculation methods using mathematical models, and parameters obtained experimentally.

Since the working cycle of the transducers under consideration lasts 1 ... 2 ms with a rapid movement of the armature, this imposes special features on carrying out experimental investigations [8].

**The goal of the paper** is a substantiation of a technique of experimental investigations of LIEC which are used as shock-power devices and electromechanical accelerators, and comparison of experimental results with the calculated parameters obtained by means of mathematical model.

**Mathematical model.** In the induction-type LIEC, excitation from the CES generates fast electromagnetic, thermal and mechanical processes that occur when the armature moves rapidly relative to the inductor winding (IW). The implementation of the mathematical model of LIEC using a chain approach based on the theory of electrical circuits does not allow us to fully describe the totality of spatial and temporal processes [7]. Proceeding from this, a mathematical model of the LIEC was developed, which is based on the field approach using the finite element method [9]. To determine the electromagnetic parameters of the LIEC in the cylindrical coordinate system  $\{r, z\}$  the vector magnetic potential  $A$  is calculated

$$\frac{\partial}{\partial r} \left( \frac{1}{r\mu(B)} \frac{\partial(rA)}{\partial r} \right) + \frac{\partial}{\partial z} \left( \frac{1}{\mu(B)} \frac{\partial A}{\partial z} \right) - \sigma \frac{\partial A}{\partial t} = 0. \quad (1)$$

where  $\mu(B)$  is the magnetic permeability depending on the magnetic flux density  $B$  of ferromagnetic material;  $\sigma$  is the yoke electrical conductivity.

Components of the magnetic flux density vector are calculated by known relations:

$$B_z = \frac{1}{r} \frac{\partial(rA)}{\partial r}; \quad B_r = -\frac{\partial A}{\partial z}. \quad (2)$$

The boundary conditions of the system is equation  $n \times A = 0$ , where  $n$  is the unit vector of the outer normal to the surface. For ferromagnetic materials nonlinear magnetization curve  $B = f(H)$  is used.

Current in the inductor is determined by using the equation:

$$(R_e + R_1) i_1 + L_e \frac{di_1}{dt} + \frac{1}{C} \int i_1 dt + \frac{N_1}{s} \int \frac{dA_l}{dt} dv = U_0, \quad (3)$$

where  $R_e$  is the active resistance of the external circuit;  $R_1$  is the IW active resistance;  $i_1$  is the IW current;  $L_e$  is the inductance of the external circuit;  $U_0$  is the CES charging voltage;  $C$  is the CES capacitance;  $N_1$  is the number of turns of the inductor;  $s$  is the cross-sectional area of the IW penetrated by the magnetic flux;  $A_l$  is the projection of the magnetic vector potential on the direction of traversal of the contour;  $V$  is the volume of the inductor.

Electrodynamical forces (EDF) acting on the yoke are determined by using the Maxwell tension tensor:

$$f_z = 0,5 \oint_S [H(B \cdot n) + B(H \cdot n) - n(H \cdot B)] ds, \quad (4)$$

where  $S$  is the area bounding the yoke cross-section;  $n$  is the unit vector of the normal to the surface of the yoke.

EDF impulse determining integral force action on the yoke is described by the expression:

$$F_z = \int_0^t f_z dt. \quad (5)$$

Mechanical processes in the LIEC at the axial yoke displacement are described by the equation

$$(m_e + m_2) \frac{dv_z}{dt} = f'_z, \quad (6)$$

where  $f'_z = f_z - k_\mu v_z - 0.125\pi\gamma_a\beta_a D_m^2 v_z^2$ ;  $m_e$  is the AE mass;  $m_2$  is the yoke mass;  $v_z$  is the yoke velocity;  $k_\mu$  is the dynamic friction coefficient;  $\gamma_a$  is the air density;  $\beta_a$  is the aerodynamic resistance coefficient;  $D_m$  is the AE external diameter.

Axial displacement  $\Delta z$  and yoke velocity  $v_z$  on each calculation step  $\Delta t$  can be represented as recurrent relations [5]

$$\Delta z(t_{k+1}) = \Delta z(t_k) + v_z(t_k) \Delta t + f'_z \Delta t^2 (m_e + m_2)^{-1}; \quad (7)$$

$$v_z(t_{k+1}) = v_z(t_k) + f'_z \Delta t (m_e + m_2)^{-1}. \quad (8)$$

Equations (1) – (8) describe electromechanical processes in LIEC at initial conditions:  $u_c(0)=U_0$ ;  $i_1(0)=0$ ;  $\Delta z(0)=0$ ;  $v_z(0)=0$ , where  $u_c$  is the CES voltage. In the calculation, we assume the absence of mechanical movements (recoil) of the inductor, the deformation of the elements, and the strictly axial disposition and movement of the yoke relative to the inductor.

To determine the heating temperature of the IW and the joke of the LIEC, we use the field model, which allows to take into account at each time step the spatial distribution of the temperatures in the active (IW and yoke) and passive elements (inductor frame, armature yoke disk) of the LIEC elements [10].

The solution of the system of equations (1) – (8) was obtained using the finite element method in integration with respect to spatial variables and the improved Gear method in time integration. When moving the joke, a «deformable» grid is used. To solve this goal, the mathematical model of LIEC was developed in the software package *Comsol Multiphysics* which allows to adaptively change the grid and to monitor errors when working with various numerical solvers [11].

The simulation of electrical processes was carried out by physical modules «Electrical circuit», which calculated the transient processes, and «Magnetic fields», which calculated the parameters on the basis of the magnetic field taking into account the displacement of the electrically conductive armature. Modeling of magnetic processes was carried out by the physical module «Magnetic fields», in which the electromagnetic process is described by a system of differential equations for each node of the grid partition. Modeling of thermal processes was carried out by the physical module «Heat transfer in solid».

The mathematical model of LIEC is realized in the following sequence:

- Physical modules («Magnetic fields», «Electrical circuit», «Heat transfer in solid», «Fluid structure interaction»), problem dimension (2D), model type (time-dependent) and calculation method are selected;
- the geometry of the LIEC is formed and the calculated areas of physical problems are determined;
- initial data are given in the form of quantities and functions describing the relationships between the parameters, for example, the dependence of the resistivity of the material on temperature;
- initial and boundary conditions for the physical problems under consideration;

– the calculated areas are discretized taking into account the geometric model of the LIEC;

– methods of solution are chosen, usually *MUMPS*, *PARDISO* and numerical calculations are performed.

The solution of the LIEC multiphysical mathematical model is produced by the *BDF* (*backward differentiation formula*) method or the *Generalized alpha* method with floating step and time constraints. This is due to a change in the value of the calculation error, depending on the selected step. The solution of the problem begins with a step in time by 6 orders of magnitude less than the maximum set step. This step automatically varies depending on convergence conditions and the relative error of the solutions obtained.

**Electromechanical processes in LIEP.** Let us consider the LIEC of an induction type of a coaxial disk configuration [12]. This LIEC consists of a fixed IW with an outside diameter  $D_{ex1} = 100$  mm, internal diameter  $D_{in1} = 10$  mm, height  $H_1 = 10$  mm and the number of turns  $N_1 = 46$ . Copper bus section  $a \times b = 1.8 \times 4.8$  mm<sup>2</sup>. The joke is made in the form of a copper disk with the following parameters: outer diameter  $D_{ex2} = 100$  mm, inner diameter  $D_{in2} = 10$  mm, height  $H_2 = 3$  mm. An impact AE with a mass  $m_e = 0.275$  kg is attached to the joke. The CES has a capacitance  $C = 2850$  μF and a charging voltage  $U_0 = 400$  V. The electronic system provides the formation of a polar aperiodic current in the IW, for which the latter is shunted by a reverse diode.

Electromechanical processes in LIEC have a complex space-time character. Fig. 1 shows the current density in the inductor  $j_1$ , the current density in the joke  $j_2$  averaged over the cross section, the EDF value  $f_z$  and the EDF impulse  $F_z$  which act on the armature, moved by a distance  $z$  with respect to the inductor with the velocity  $v_z$ . After  $t = 1.2$  ms after the start of the working process, the current in the armature changes polarity, which causes the following character of the force action: the initial repulsion is replaced by the subsequent attraction.

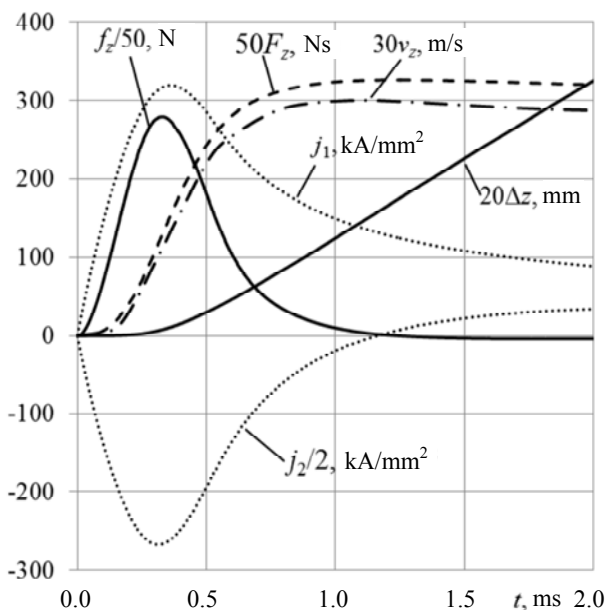


Fig. 1. Electromechanical characteristics of LIEC

The process of moving the joke begins after a certain time after the start of the work process. At each time step, an appreciable uneven distribution of the flux density of the magnetic field  $B$  in the active elements of the LIEC is observed (Fig. 2,*a*). The greatest concentration of the field is observed in the region between the IW and the joke. However, this occurs only at certain points in time, for example, at the time of the maximum EDF. In the following, the maximum induction of the magnetic field decreases and moves to the central part of the inductor.

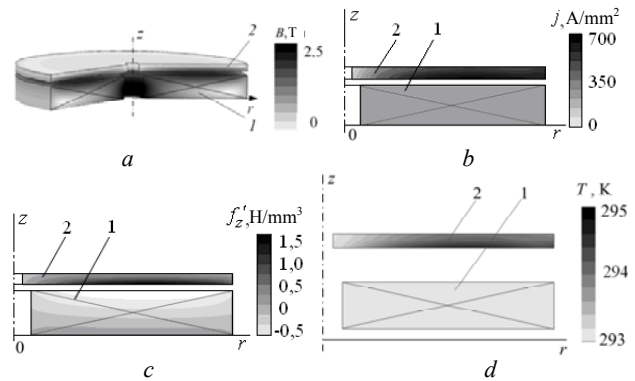


Fig. 2. Distribution of the magnetic fields (*a*) and current densities (*b*) and specific axial forces (*c*) at the instant of the maximum of the EDF and the distribution of the thermal field at the end of the working cycle (*d*): 1 – IW; 2 – joke

When the LIEC is operating at each instant of time, there is a significant spatial unevenness in the density of the induced current in the armature (Fig. 2,*b*). Specific EDF  $f_z'$  unevenly affect both the joke and the IW (Fig. 2,*c*). In this case, the temperature gradients  $T$  in the joke are insignificant, and in the IW practically absent in 1 ms after the start of work with one working cycle (Fig. 2,*d*).

When the LIEC works as an accelerator, it is first of all necessary to control the movement of the armature, and when operating as a shock-power device, it is necessary to force the relevant object.

In the experimental investigations, electrolytic capacitors HJ with a nominal voltage  $U_0 = 450$  V and capacitances  $C = 150$  μF and  $C = 330$  μF were used.

The method of carrying out the experimental research of the LIEP is that simultaneously the electric parameters (current in the IW) and the mechanical parameters characterizing the power and velocity parameters of the joke with IE are registered. Power indicators, first of all, are important for shock-power devices, and high-speed ones for electromechanical accelerators.

Power indicators were studied using piezoelectric sensors, a strain gage system, a pressure pulsation sensor, and high-speed video recording. Velocity indicators were investigated with the help of a resistive displacement sensor, which allows recording the character of the armature movement with AE at each moment of time.

#### Investigations of LIEC as a shock-power device.

**Investigations using piezoelectric sensors.** For experimental investigations of the LIEC operating as a shock-power device, a device was developed that includes

an inductor 1 containing IW, which, with the help of an epoxy resin, is padlocked in a glass-textolite frame (Fig. 3).

The inductor is attached to the support plate 2. A steel impact wheel 4 is connected to the armature 3, which acts on a vertically mounted striker 5 made of steel 70, striking the upper steel plate 6. The support plate 2 is fixed to the lower steel plate 7. The plates 6 and 7 are connected to each other by means of adjustable supports 8, which makes it possible to vary the working stroke of the striker  $Z_e$ . Springs 9 provide the given force of counteraction to movement. On the plate 6, limiting the working stroke of the striker 5, a piezo-sensor 10 is installed on top, which converts the mechanical vibrations that occur when the striker strikes the electric signals, transmitting them to the noise and vibration meter BИИВ-003. The meter converts the electric signals of the piezoelectric sensor into the values of vibration acceleration  $a_f$  and the vibration velocity  $v_f$ . In the LIEC study, the current in the IW and the vibration of the plate 6 are measured simultaneously using a two-channel electronic oscilloscope RIGOL DS 522M.

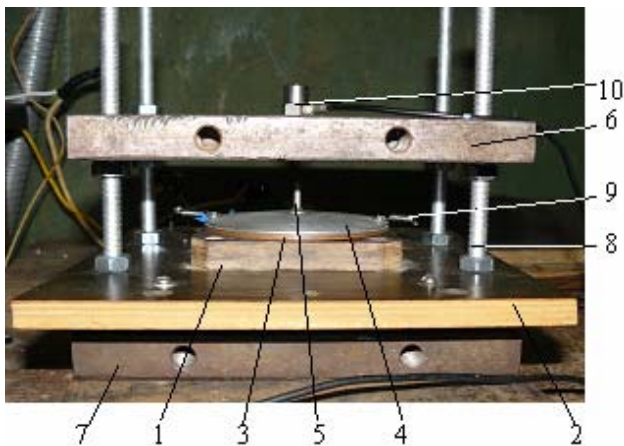


Fig. 3. Experimental installation for the investigation of LIEP using a piezoelectric sensor

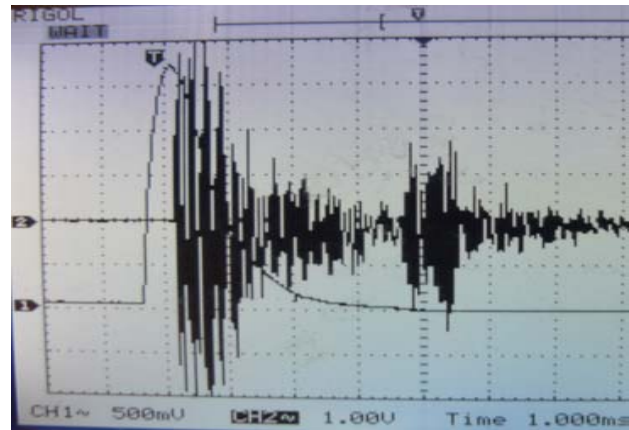
In Fig. 4 shows the oscillograms of the currents of IW  $i_1$  and vibration acceleration  $a_f$  for different values of the working stroke of the joke  $Z_e$ .

In the absence of the joke travel, the vibration of the upper plate, detected by the sensor, occurs with a certain delay  $t_0$  with respect to the instant of the current in the IW. As the value of the working stroke  $Z_e$  increases, the delay time of the vibrational processes of the upper plate increases with respect to the instant of the current in the IW  $t_z$ .

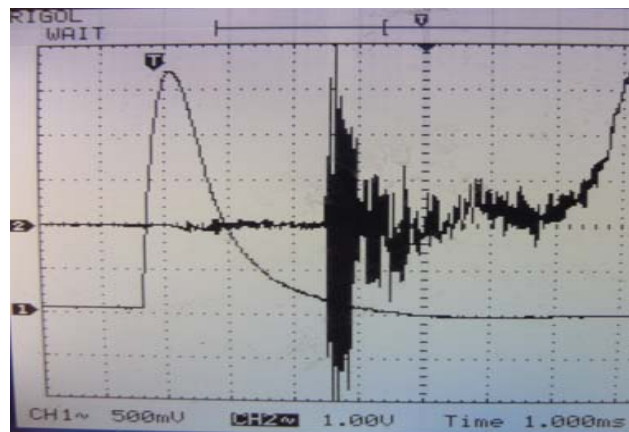
On the basis of experimental investigations, it is determined:

- form  $i_1$  and amplitude value  $I_{1m}$  of the current of the IW;
- duration of the edge of the current pulse of the IW  $t_{fr}$ ;
- duration of the current pulse of the IW  $t_{pul}$ ;
- delay time of vibration of the upper plate in relation to the moment of occurrence of the current of the IW  $t_z$ ;
- average joke velocity with AE  $V_0 = Z_e(t_z - t_0)^{-1}$ ;

- the value of vibration acceleration  $a_f(t)$  proportional to the instantaneous force  $f_z(z, t)$  acting on the upper plate;
- the value of the vibration velocity  $v_f(t)$  proportional to the momentum  $F_z$  acting on the upper plate.



a



b

Fig. 4. Oscillograms of current in the IW (channel CH1) and vibration acceleration (channel CH2) with the value of the working stroke  $Z_e$ : 0 mm (a); 10 mm (b)

The measured values of the average speed of the joke with the AE  $V_0$  for different values of the working stroke of the joke  $Z_e$  are 8 to 15% less than the calculated ones, which can be explained not by complete consideration of all opposing and braking forces. Analogous dependencies appear between the calculated and experimental values of the EDF pulse  $F_z$  (Fig. 5).

Thus, the largest values of the EDF pulse  $F_z$  arise when the joke is locked, then they decrease practically linearly with the increase in the working stroke of the joke  $Z_e$ . Both experimental and calculated dependences practically linearly increase with increasing voltage  $U_0$ , and the current amplitude of the IW  $I_{1m}$  in the presence of the joke increases.

The influence of the shape of the joke, the parameters of the CES, the working stroke  $Z_e$ , the initial gap  $\Delta Z_0$  between the joke and the inductor, and the accelerated mass on the LIEC indicators were studied experimentally. It is established that when the round armature is used in comparison with the rectangular joke, the processes change as follows: the maximum value of the EDF  $f_z$  increases by 25%, the amplitude of the current

of the IW  $I_{1m}$  increases by 5%, and the duration of the IW current pulse  $t_{pul}$  and the time delay  $t_z$  decrease by 10%. This indicates a greater efficiency of the round joke than the rectangular one.

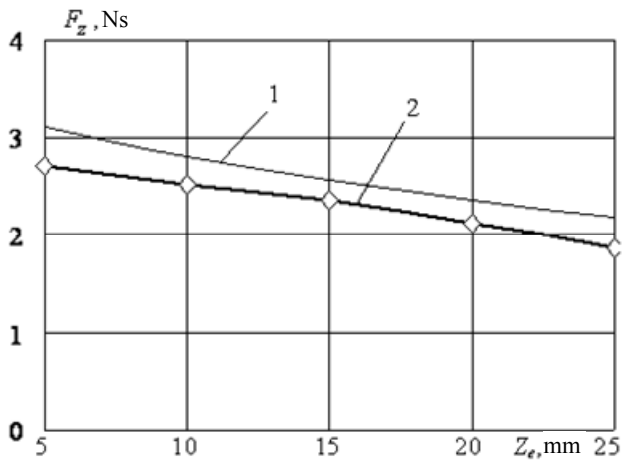


Fig. 5. Dependences of the calculated (1) and measured (2) values of the EDF pulse on the joke stroke

With an increase in the voltage of the CES, the amplitude of the current of the IW increases by more than 2 times, the amplitude of the vibrative acceleration  $a_{vib}$ , and therefore the instantaneous value of the EDF  $f_z$  acting on the upper plate, increases almost 5 times. The delay time  $t_z$  decreases from 0.7 to 0.5 ms.

As the working stroke  $Z_e$  increases, the delay time  $t_z$  of the vibration of the upper plate increases with respect to the beginning of the current pulse of the IW which leads to a decrease in the EDF amplitude  $f_z$ . On oscillograms, an insignificant vibration of the upper plate, which occurs before the impact of the striker, is caused by the return of the inductor transmitted through the adjustable supports (Fig. 4,b).

Fig. 6 shows the effect of capacitance  $C$  at different voltages  $U_0$  of the CES on the amplitude of the current of the IW  $I_{1m}$  of the LIEC. The experimental and calculated values of the current amplitude increase with increasing capacitance  $C$ : with an increase in capacitance by a factor of 2 (from 2000 to 4000  $\mu\text{F}$ ), the current increases by 17%. Moreover, the amplitude of the current of the IW  $I_{1m}$  is higher, the higher the voltage  $U_0$ . The growth of  $I_{1m}$  values is more significant in the range of capacitances  $C = 2000 \dots 3000 \mu\text{F}$ .

The magnitude of the voltage  $U_0$  of the CES slightly affects the duration of the edge of the current pulse of the IW  $t_{fr}$ . The front duration remains practically unchanged for different  $U_0$  and fixed values of the capacitance  $C$  of the CES. Fig. 6,b shows the effects of the CES capacitance on the duration of the edge of the current pulse of the IW  $t_{fr}$  in the presence and absence of the joke in the LIEC. Both the experimental and calculated values of the duration of the front of the current of the IW increase with an increase in the capacity of the CES  $C$ , having practically the same regularity. And the duration of the current front of the IW  $t_{fr}$  is higher in the LIEC without joke.

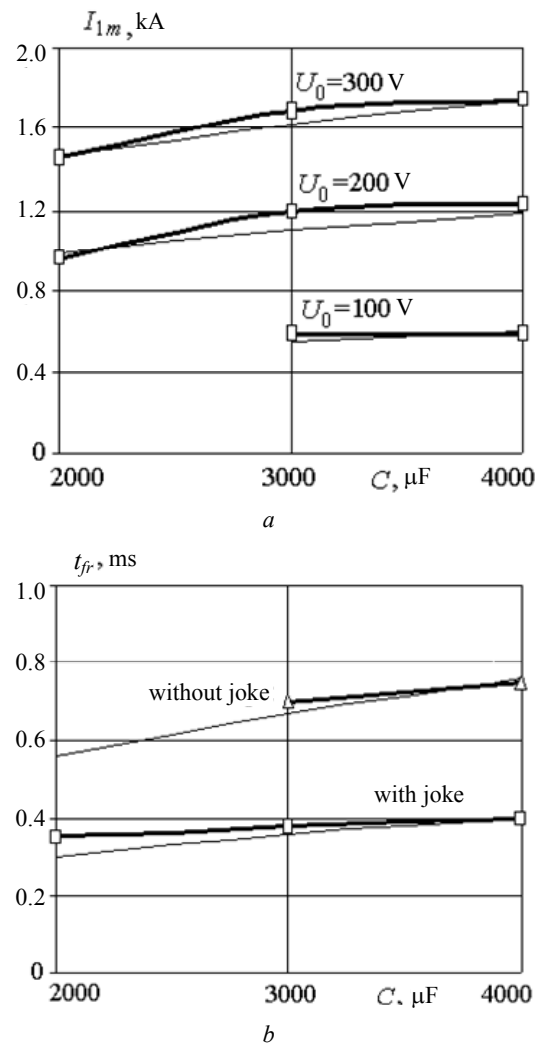


Fig. 6. Dependence of experimental (fat lines) and calculated (fine lines) values of the amplitude (a) and the duration of the front (b) of the IW LIEC current from the CES capacitance

The efficiency of the LIEC is significantly influenced by the initial gap between the joke and the inductor  $\Delta Z_0$  (Fig. 7). With increasing clearance  $\Delta Z_0$ , the magnetic coupling between the joke and the IW decreases, and hence the influence of the armature on the current of the IW  $i_1$  decreases, which leads to a decrease in the amplitude of the current  $I_{1m}$ .

The larger the initial clearance, the greater the IW current curve becomes similar to the IW current curve in the absence of the joke (the magnetic coupling of the inductor to the joke is zero). An increase in the initial gap  $\Delta Z_0$  leads to a significant decrease in the EDF pulse. Fig. 7,b shows the dependence of the experimental and calculated values of the EDF pulse on the initial gap when using the CES with parameters  $C = 3000 \text{ V}$ ,  $U_0 = 200 \text{ V}$ .

With an increase in the initial gap  $\Delta Z_0$  between the armature and the inductor by a factor of 2 from 2.5 to 5 mm, the amplitude of the current in the IW  $I_m$  decreases by 8%, the duration of the current pulse in the IW  $t_{pul}$  increases by 6%, and the edge of the current pulse in the IW  $t_{fr}$  by 8%. At the same time, the magnitude of the vibration acceleration  $a_{vib}$ , and hence the EDF  $f_z$  decreases by 25%, the time delay  $t_z$  increases almost 2 times. As the  $\Delta Z_0$  increases from 0 to 5 mm, the value of the force pulse

decreases by 54%. This indicates that the initial gap between the inductor and the joke must be chosen as small as possible.

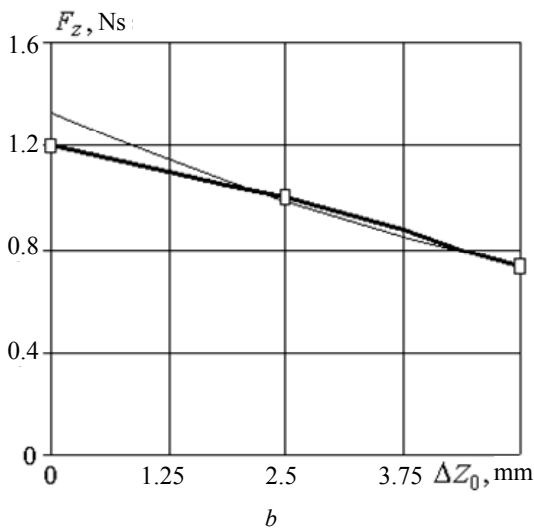
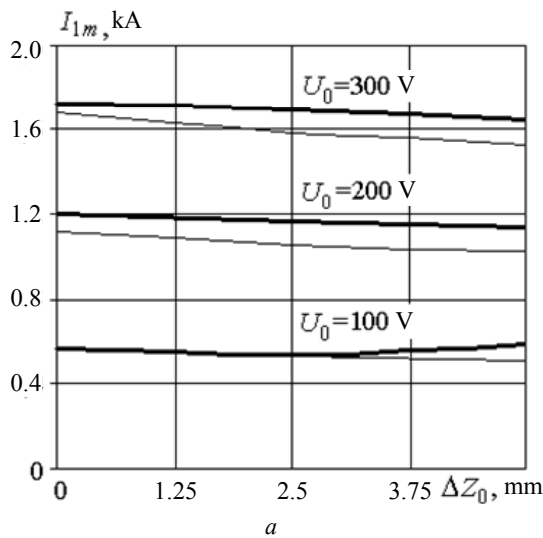


Fig. 7. Dependence of the experimental (thick lines) and calculated (fine lines) values of the current amplitude in the IW (a) and the EDF pulse (b) on the initial gap between the inductor and the joke

Fig. 8 shows the experimental and calculated values of the average velocity of the joke  $V_0$  in the section of the working path  $Z_e$  at  $C = 7000 \mu\text{F}$ , but different voltages  $U_0$  of the CES. The calculated velocity is somewhat higher than the experimental one, which can be explained by the more complex nature of the real aerodynamic resistance, compared with the mathematical model, not fully taking into account all the opposing forces and the presence of the inductor yield.

As the capacity of the CES  $C$  decreases 2.2 times (from 6270 to 2859  $\mu\text{F}$ ), the electrical processes change as follows: the amplitude of the current in the IW  $I_m$  decreases by 28%, the duration of the current pulse in the IW  $t_{pul}$  by 71%, the edge of the current pulse in the IW  $t_{fr}$  by 43%. As a result, the delay time  $t_z$  decreases by 14%, and the magnitude of the EDF pulse  $F_z$  by 3.12 times.

In general, the conducted experimental investigations using piezoelectric sensors are in

satisfactory agreement with the theoretical results. They showed that it is possible to effectively record the indicators of the force impact of the LIEC on the object, which is important for shock-power devices.

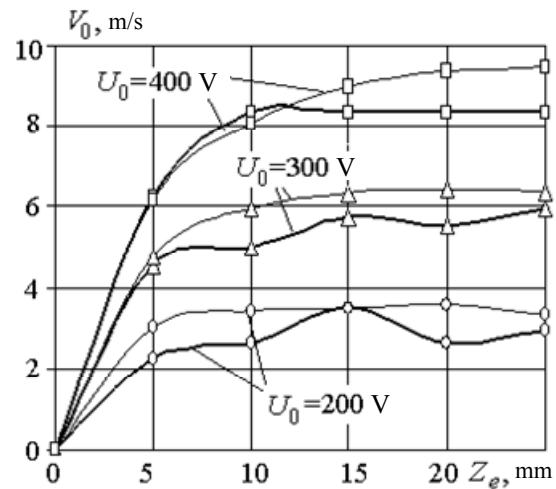


Fig. 8. Experimental (fat lines) and calculated (thin lines) dependence of the average velocity on the displacement of the LIEC joke

**Study using strain sensors.** Consider the effectiveness of the use of strain sensors for recording force effects on an object. An experimental stand for the investigation of the LIEC, operating as a shock-power device, is shown in Fig. 9,a. LIEC is attached to an insulating base plate, which is mounted on vertical adjustable supports. With these supports, it is possible to change the height of the support plate, thus setting the joke travel with firing  $Z_e$ .

LIEC provides for the movement of the joke with the striker vertically downwards before colliding with the object of impact—a shock steel plate with dimensions of  $0.18 \times 0.18 \times 0.006 \text{ m}^3$  (Fig. 9,b). The shock plate on the reverse side is covered with a network of strain gauges, united in rosettes. The wires from the sensors are led out through the holes in the plate, which is fixed to the support frame. These sensors form five groups symmetrically located relative to the point of impact, with each group containing three sensors, one side of which forms a node, and the other sides – rays at an angle of  $45^\circ$  to each other (Fig. 9,c). The stand contains a replaceable shock plate holder, which allows to realize different types of fastening: articulated, rigid and free support.

A bridge circuit was used to measure the resistance of strain gauges. A differential signal receiver is used to measure the voltage drop.

During the experiments, information and measuring complex was used to record deformation processes in the target [13]. The complex contains a strain gage sensor, a stabilized power supply, a conjugation and protection unit, an ADA-1406 ADC and a personal computer. The digital data received from the ADC board is delivered to the computer, where it is processed using special software. It allows you to record a signal, determine the values of the measured parameters, the signal spectra and the decay

time of the oscillations. As a receiver in the sensor signal generation unit, a precision instrument amplifier AD623 is used, which allows to suppress the common-mode interference coming to the input along with the useful signal. The start-up of the test facility takes place remotely simultaneously with the commencement of the tests.

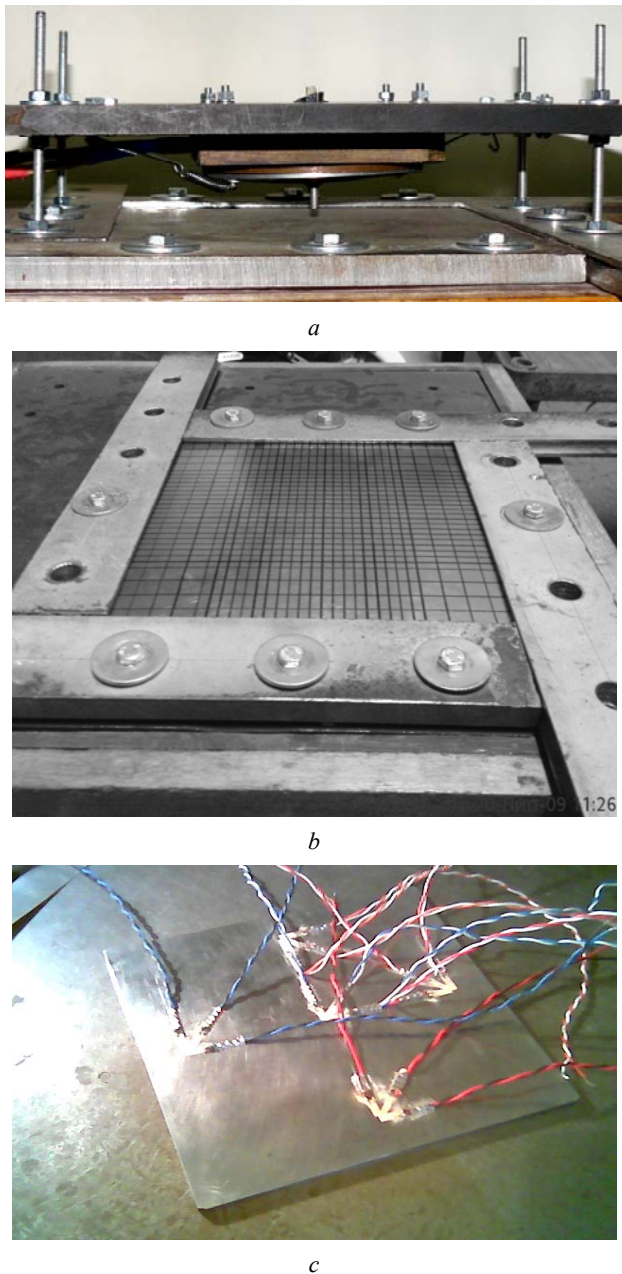


Fig. 9. Experimental installation for the investigation of LIEC using strain sensors (a) and object of effects – steel plate with strain sensors: top view (b) and bottom view (c)

During the operation of the LIEC, intensive magnetic fields are excited which generate load cell signals proportional to the axial component of the field at their location. Thus, in the absence of deformation processes in the shock plate, the magnetic field of the LIEC generates the background signals of the strain sensors, whose amplitudes increase with increasing voltage  $U_0$  (Fig. 10).

It has been experimentally established that the impact of the striker along the center of the shock plate does not cause plastic deformations in it. A series of shock effects was performed, on the basis of which the average value of the amplitude of the signal, taken from the central «socket» of the shock absorber strain sensors, was determined. Subtracting the background level from the signal values, we get the value of the deformation of the shock plate. In Fig. 11 circles show outbursts of strain sensor signals on oscillograms that correspond to the deformation processes caused by impact forces of the LIEC striker on the plate.

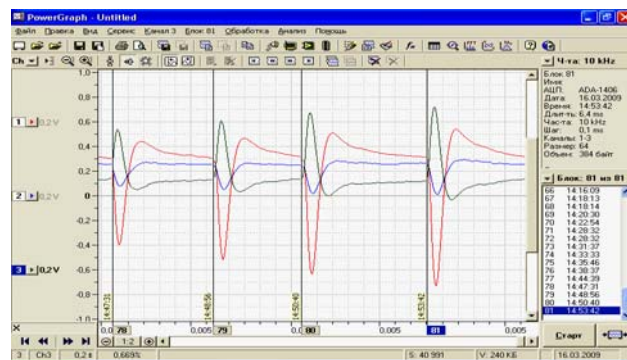


Fig. 10. Background signals of strain sensors induced by magnetic field at voltages  $U_0$ : 250; 300; 350; 400 V (from left to right)

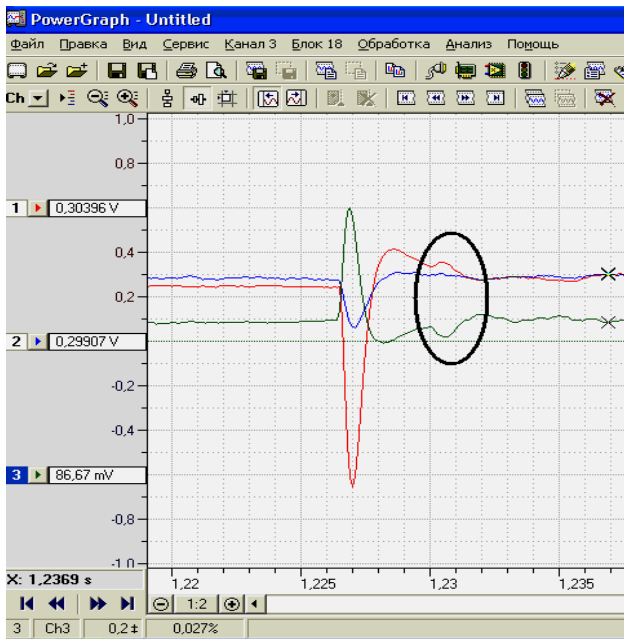
The averaged value of the maximum values of these bursts corresponds to the maximum EDF value  $f_z$  acting on the shock plate (1 mV signal is equivalent to the power load of 8.936 N). The duration of the shock pulse  $t_{pul}$  is determined by the duration of the first burst of the signal.

As the voltage  $U_0$  of the CES is increased in these experiments, as in the case of a piezoelectric sensor, the amplitudes of the IW and joke currents (background signals of the magnetic field), the size of the shock plate deformation, and the delay time between the electric and deformation processes  $t_z$  are increased.

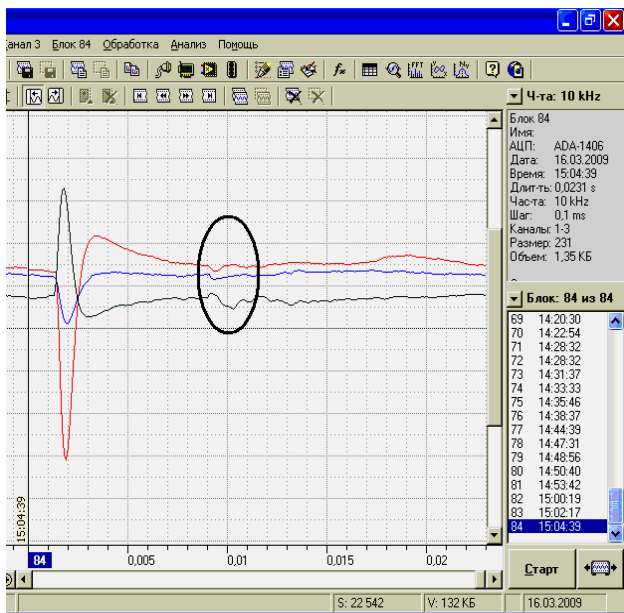
It has been experimentally established that the EDF pulse  $F_z$  decreases with increasing work path  $Z_e$  at  $U_0 = \text{const}$  and increases with an increase in the voltage of the CES  $U_0$  at  $Z_e = \text{const}$ . At the LIEC, from the beginning of the current pulse of the IW (electromagnetic processes) to the interaction of the striker accelerated by the joke, with the shock plate (mechanical processes), there is a lag of  $t_0 = 0.5$  ms at  $C = 2850 \mu\text{F}$  and  $U_0 = 300 \dots 350$  V and  $Z_e = 0$ .

Experimental studies were carried out to determine the average velocities of the joke  $V_0$  in the section of the working stroke  $Z_e$  at different voltages  $U_0$ . The resulting average velocity of the joke at voltage of 200 V was 5.1 m/s which is in satisfactory agreement with the results of the calculation.

Thus, strain sensors allow recording not only the beginning and value of the force action, but also its duration. In general, the experimental results obtained using piezoelectric and strain sensors are in good agreement with each other.



a



b

Fig. 11. Strain sensors signals at  $U_0 = 350$  V,  $C = 2850 \mu\text{F}$ ,  $Z_e = 10$  mm (a),  $Z_e = 25$  mm (b)

### Investigation of the cyclic shock impact of LIEC on a thin steel plate.

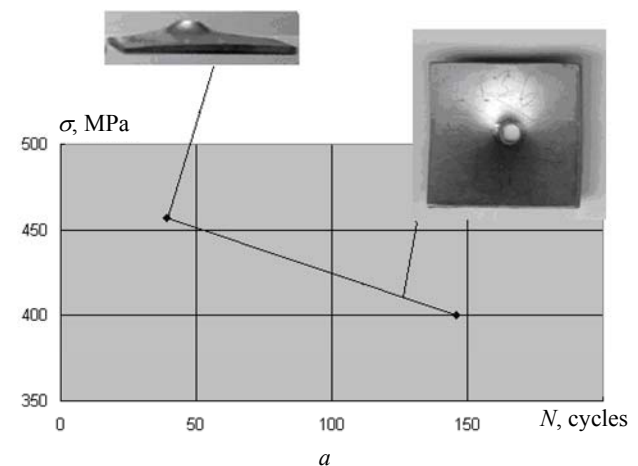
Experiments were conducted to penetrate thin (1.5 mm) stainless steel plates. With a voltage of the CES of  $U_0 = 200$  V in this plate, the value of mechanical stresses is 93.4 MPa, and when  $U_0 = 400$  V – 186.8 MPa. For a thin sheet of 12X18H10T steel, the yield strength is  $\sigma_T = 205$  MPa. Thus, at a voltage of the CES  $U_0 = 400$  V, the mechanical stresses in the plate are at the boundary of the yield point. To study the impact of the LIEC on this plate, a low-cycle shock loading was used and the average value of the number of cycles  $N$  was determined before the plate was pierced by the striker.

For the first group of experiments in which a load with stress value of 400 MPa was realized,

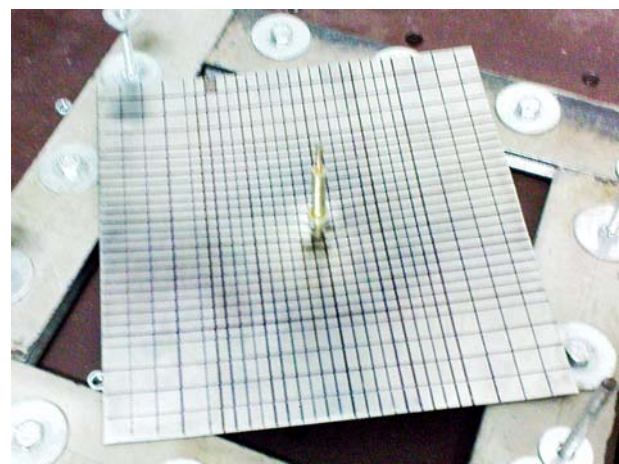
$N = 146$  cycles, and for the second group, at a voltage of 457 MPa,  $N = 39$  cycles. When punching, a bulge (cork) with a diameter of 4 mm and a thickness of 1.1 mm was formed with even edges.

Fig. 12,a shows the experimental curve of the low-cycle impact strength and photographs of a thin steel plate deformed at the corresponding values of the mechanical stresses. Fig. 12,b shows a photo of a plate pierced by a striker. As a result of several experiments during the cyclic operation of the LIEC, it was found that the average number of cycles before punching the plate was  $N = 79$ .

**Investigations using videorecording.** At the test bench for the LIEC investigations using strain sensors, measurements were made of the instantaneous velocity of the joke with a striker using a video camera with a digital camera. After the shooting, the recording was processed and its decomposition into separate frames (Fig. 13). In this case, the time was determined for which the joke with the striker passes the distance to the shock plate. On average, the time from the detachment of the joke to the contact of the striker with the shock plate was 9.65 ms. The distance from the end of the striker to the shock plate in this experiment is 5 mm. Consequently, the average speed in the section of the working stroke was 5.18 m/s which is in satisfactory agreement with the results of the experiments described above.



a



b

Fig. 12. The low-cycle impact strength curve (a) and a thin steel plate pierced by the LIEC striker (b)





a



b

Fig. 13. Outcomes of videorecording at the beginning (a) and at the end (b) of the operation process

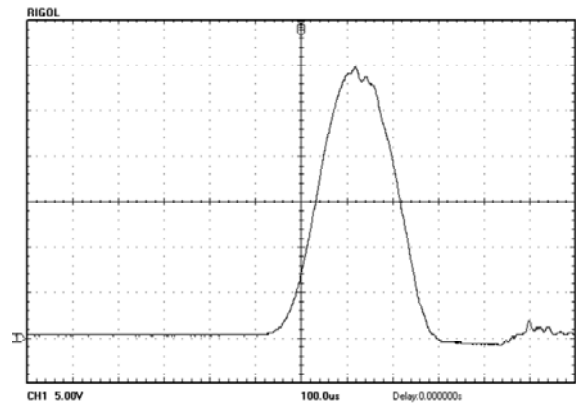
**Investigations using a pressure pulsation sensor.**

A piezoelectric pressure pulsation sensor M101A06 by the PCB Company (USA) was used to measure the dynamic pressure exerted by the striker on the shock plate (Fig. 14).

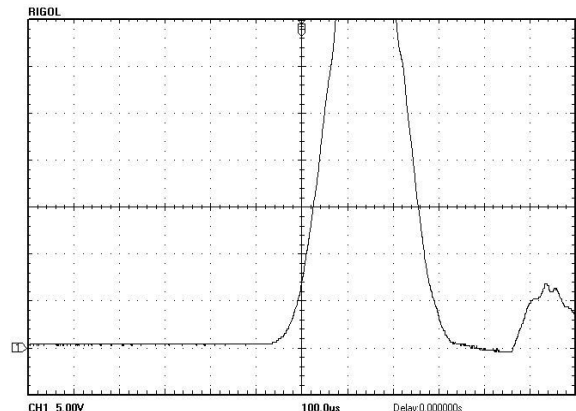


Fig. 14. External view of the piezoelectric sensor of pressure pulsations M101A06 by the PCB Company

The sensor is equipped with an integrated amplifier, has dynamic range of 0.68-3450 kPa, sensitivity of 1.45 mV / kPa and frequency range of 0.01-130000 Hz. The sensor withstanding maximum pressure of 34.5 MPa contains a built-in ICP amplifier (ICP – *Integrated Circuit Piezoelectric*). The sensor readings were recorded using an electronic oscilloscope RIGOL (Fig. 15).



a



b

Fig. 15. Oscillograms of dynamic pressure on the shock plate with voltage of the CES 300 V (a) and 400 V (b)

In these experiments, the shape, size, and duration of the force pulse in the shock plate were determined upon the action of the LIEC striker on it. The results of these studies are in satisfactory agreement with both the calculated EDF values (Fig. 1) and the results of the experiments described above.

**Investigations of LIEC as an electromechanical accelerator.** To investigate the LIEC operating as an electromechanical accelerator, it is necessary to measure the movements of the armature at each instant of time in the working area. For this purpose, the installation shown in Fig. 16 was developed. LIEC inductor 1 consists of a multi-turn winding wound from a copper bus in two layers and hardened with an epoxy resin. A steel shock wheel 3 is attached to the joke 2. The inductor is connected to the CES by way of the current leads 4. To measure vertical movements, a resistive sensor 5 fixed to the C-shaped frame 6 is used.

Between the horizontal walls of the frame 6 is movably installed a guide rod 7 passing through the central holes of the inductor and the armature. The inductor is mounted on a nonmetallic base 8 on the bottom wall of the frame, and a resistive displacement sensor is mounted on the top wall of the frame 5. A damper spring is attached to the top wall of the frame (not shown in the photo). The guide rod is connected to the shock disk and the movable contact of the displacement sensor, the signal from which is fed to the electronic oscilloscope. In this way, the current in the

inductor  $i_1$  and the displacement  $\Delta z$  of the armature with the steel shock disk and the guide rod are measured simultaneously (Fig. 17).

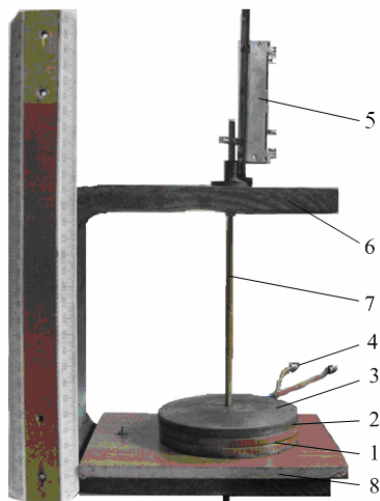


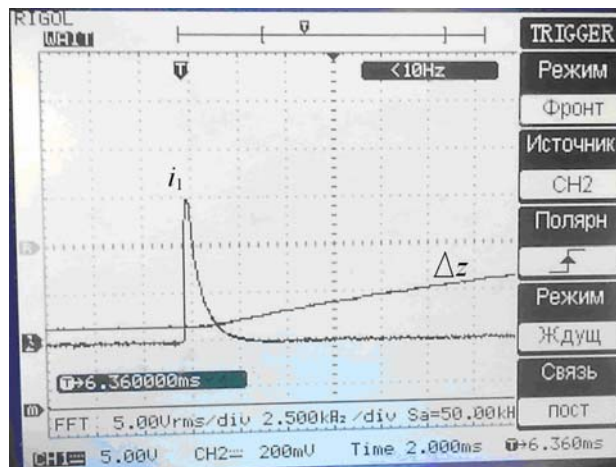
Fig. 16. General view of the experimental setup for investigations of LIEC working as an accelerator with steel power disk

It has been experimentally established that the movement of the armature begins with a delay in relation to the moment of occurrence of the current pulse and is practically linear in the initial part of the acceleration. At an increased voltage of the CES  $U_0 = 400$  V, the movement of the armature after the passage of the initial segment slows down, which is due to its interaction with the damper spring.

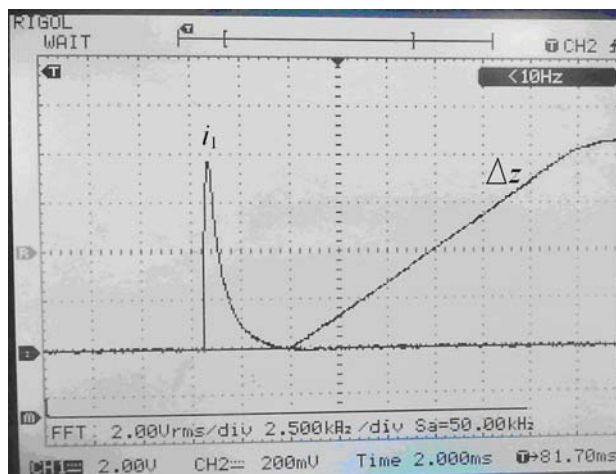
The impact of the impact disk material on the performance of the electromechanical accelerator was studied. In the experiments we used steel (Fig. 16) and ceramic (Fig. 18) impact discs.

As investigations have shown with the use of a ceramic power disk, the pulse duration of the current of the IW increases by 11%, and its magnitude by 15%. At the same time, the joke velocity increases by 3% after 1.5 ms, and after 5 ms – by 7%. Thus, a ceramic power disk is more efficient than a steel disk, although its manufacturing technology and operating conditions are more complex.

In general, the results of the LIEC investigations as an electromechanical accelerator are in satisfactory agreement with the calculated parameters: electrical parameters (current in the IW) – to 4%, and mechanical indicators (joke velocity) – with accuracy of 9%.



a



b

Fig. 17. Oscillograms of the current of the inductor  $i_1$  and the displacement of the yoke  $\Delta z$  at the voltage of the CES 300 V (a) and 400 V (b) using a steel power disk



Fig. 18. General view of the experimental setup for investigations of LIEC working as an accelerator with ceramic power disk

## Conclusions.

A technique for experimental research has been developed, which consists in the simultaneous recording of electrical and mechanical parameters characterizing the power and velocity indicators of the LIEC.

A mathematical model of the LIEC of induction type is developed, which describes fast electromagnetic, thermal and mechanical processes that appear when the joke moves relative to the inductor.

It is shown that the electromechanical processes in the LIEC have a complex spatial and temporal character, and at each instant of time, an appreciable spatial unevenness of the current density induced in the joke is observed.

Power indicators are recorded using a piezoelectric sensor, a system of strain sensors, a pressure pulsation sensor and high-speed videorecording, and velocity indicators using a resistive displacement sensor.

The results of experimental investigations are in satisfactory agreement with the results of calculations obtained with the help of a mathematical model.

## REFERENCES

1. Bissal A. *Licentiate thesis on the design of ultra-fast electro-mechanical*. Stockholm, Sweden. 2013. 120 p.
2. D.-K. Lim, D.-K. Woo, I.-W. Kim, D.-K. Shin, J.-S. Ro, T.-K. Chung, H.-K. Jung. Characteristic Analysis and Design of a Thomson Coil Actuator Using an Analytic Method and a Numerical Method. *IEEE Transactions on Magnetics*, 2013, vol.49, no.12, pp. 5749-5755. doi: 10.1109/tmag.2013.2272561.
3. Bolyukh V.F., Vinnichenko A.I. Concept of an induction-dynamic catapult for a ballistic laser gravimeter. *Measurement Techniques*, 2014, vol.56, iss.10, pp. 1098-1104. doi: 10.1007/s11018-014-0337-z.
4. Bolyukh V.F., Luchuk V.F., Rassokha M.A., Shchukin I.S. High-efficiency impact electromechanical converter. *Russian electrical engineering*, 2011, vol.82, no.2, pp. 104-110. doi: 10.3103/s1068371211020027.
5. Bolyukh V.F., Shchukin I.S. *Lineinye induktsionno-dinamicheskie preobrazovateli* [Linear induction-dynamic converters]. Saarbrücken, Germany, LAP Lambert Academic Publ., 2014. 496 p. (Rus).
6. Podoltsev A.D., Kucheriava I.N. *Mul'tifizicheskoe modelirovanie v elektrotekhnike* [Multiphysical modeling in electrical engineering]. Kyiv: Institute of Electrodynamics of NAS of Ukraine, 2015. 305 p. (Rus).
7. L. Shoubao, R. Jiangjun, P. Ying, Z. Yujiao, Z. Yadong. Improvement of Current Filament Method and Its Application in Performance Analysis of Induction Coil Gun. *IEEE Transactions on Plasma Science*, 2011, vol.39, no.1, pp. 382-389. doi: 10.1109/tps.2010.2047276.
8. Bolyukh V.F., Oleksenko S.V., Schukin I.S. Experimental study of ferromagnetic core parameters influence on electromechanical characteristics of a linear induction-dynamic converter. *Electrical engineering and electromechanics*, 2014, no.5, pp. 13-18. (Rus). doi: 10.20998/2074-272X.2014.5.02.
9. Bolyukh V.F., Oleksenko S.V. The influence of the parameters of a ferromagnetic shield on the efficiency of a linear induction-dynamic converter. *Russian Electrical Engineering*, 2015, vol.86, no.7, pp. 425-431. doi: 10.3103/s1068371215070044.
10. Bolyukh V.F., Shchukin I.S. The thermal state of an electromechanical induction converter with impact action in the cyclic operation mode. *Russian electrical engineering*, 2012, vol.83, no.10, pp. 571-576. doi: 10.3103/s1068371212100045.
11. Comsol Multiphysics modeling and simulation software. Available at: <http://www.comsol.com> (accessed 05 May 2015).
12. Bolyukh V.F., Luchuk V.F., Rassokha M.A., Shchukin I.S. High-efficiency impact electromechanical converter. *Russian electrical engineering*, 2011, vol.82, no.2, pp. 104-110. doi: 10.3103/s1068371211020027.
13. Naumov I.V., Bolyukh V.F., Breslavskiy D.V. Deformation and fracture of the plates during loading cylindrical drummer. *Mechanics and engineer*, 2010, no.1, pp. 207-216. (Rus).

Received 30.11.2016

V.F. Bolyukh<sup>1</sup>, Doctor of Technical Science, Professor,  
A.I. Kocherga<sup>1</sup>, Postgraduate Student,  
S.V. Oleksenko<sup>2</sup>, Candidate of Technical Science,  
I.S. Schukin<sup>3</sup>, Candidate of Technical Science, Associate  
Professor,

<sup>1</sup> National Technical University «Kharkiv Polytechnic Institute»,  
2, Kyrpychova Str., Kharkiv, 61002, Ukraine,  
phone +38 057 7076427, e-mail: bolukh@kpi.kharkov.ua

<sup>2</sup> Joint-stock company «Kharkivoblenergo»,  
149, Plekhanovskaia Str., Kharkiv, 61037, Ukraine,  
phone +38 057 7312486, e-mail: oleksenko\_sergii@mail.ru

<sup>3</sup> Firm Tetra, LTD,  
2, Kyrpychova Str., Kharkiv, 61002, Ukraine,  
phone +38 057 7076427, e-mail: tech@tetra.kharkiv.com.ua

## How to cite this article:

Bolyukh V.F., Kocherga A.I., Oleksenko S.V., Schukin I.S. A technique of experimental investigations of linear impulse electromechanical converters. *Electrical engineering & electromechanics*, 2017, no.2, pp. 18-28. doi: 10.20998/2074-272X.2017.2.03.